J Mater Sci (2006) 41:7088–7095
DOI 10.1007/s10853-006-0934-6

Processing, crystallization and characterization of polymer derived nano-crystalline Si–B–C–N ceramics

Ravi Kumar · Y. Cai · P. Gerstel · G. Rixecker · F. Aldinger

Received: 9 July 2005 / Accepted: 8 December 2005 / Published online: 6 October 2006

Abstract Si–B–C–N ceramics were synthesized from boron modified poly(vinyl)silazanes with the chemical formula $(B[C_2H_4–Si(CH_3)NH]_3)_n$. The originally amorphous materials are crystallized at temperatures in the order of 1,800–1,900 °C, which results microstructures with grain sizes significantly below 100 nm. Several parameters of the heat treatment, including temperature, holding time and atmosphere, affect the resulting nanostructures. This and the chemical and phase composition were studied via X-ray diffraction (XRD), transmission electron microscopy (TEM), electron spectroscopic imaging (ESI) and spectrochemical analysis in order to gain an understanding of the mechanisms, which control the crystallization behavior. Ceramic samples were also produced using different particle sizes of the precursor polymer in order to quantify the effect of the varying specific surface on the crystallization behavior.

R. Kumar (✉) · Y. Cai · P. Gerstel · G. Rixecker · F. Aldinger
Max-Planck Institut für Metallforschung and Institut für Nichtmetallische Anorganische Materialien, Universität Stuttgart, Pulvermetallurgisches Laboratorium, Heisenbergstrasse 3, D70569 Stuttgart, Germany
e-mail: kumar@mf.mpg.de

Present Address:
Y. Cai
Department of Materials Science and Engineering, Georgia Institute of Technology, Atlanta, USA

Introduction

Boron modified silicon carbonitrides (Si–B–C–N) synthesized by the thermolysis of siliconorganic polymers have invoked interest in recent years because of the extraordinary properties this class of ceramics exhibits in terms of chemical, thermal and mechanical stability [1–7]. Commonly, as-thermolyzed Si–B–C–N materials are amorphous and as such metastable. Therefore, they can be converted into a more stable crystalline state upon heat treatment at temperatures above ~1,700 °C. Several studies have indicated an interesting potential of the crystallized ceramics as well [8, 9]. However, in any case optimum processing conditions are crucial for obtaining materials with the desired characteristics [10]. Janakiraman et al. [11] studied amorphous Si–B–C–N samples obtained by thermolysis of a polyborosilazane having the chemical formula $(B[C_2H_4Si(H)NH]_3)_n$. They were isothermally annealed in the temperature regime of 1,400–1,800 °C for holding times 3–100 h. The surface morphology, crystallization behavior and microstructural changes of the annealed powder samples were investigated using high resolution and energy filtering transmission electron microscopy (HRTEM, EFTEM). These investigations revealed for example, that higher surface areas of the starting polymer powders promote vapor-phase decomposition reactions during thermolysis and crystallization heat treatments resulting in SiC whisker growth. In coarser powders, the influence of the surface was manifested as a core/skin effect. The ''skin'' had undergone a higher degree of decomposition, which was accompanied by enhanced SiC crystal growth as compared to the ''core.'' Furthermore, an EFTEM investigation by Zern et al. [12] on a material annealed at 1,800 °C for 10 h showed that the

individual ceramic particles developed internal cracks on a macroscopic scale. On the crack surfaces, a layer of carbon was found. In the crack-free regions, the material was composed of Si_3N_4 and SiC nano-crystallites embedded in a turbostratic B–N–C matrix. A detailed study of the phase distribution beneath the crack surfaces showed that the first Si_3N_4 crystallites occur at a distance of approximately 5 mm from the cracks. In the immediate vicinity of the carbon covered crack surfaces, silicon nitride was locally decomposed with formation of silicon carbide.

In this paper, an attempt is made to optimize the processing parameters for the production of dense bulk samples of the ceramics as a function of the size distribution of the polymer particles. This includes careful analysis of the structure of Si–B–C–N ceramics crystallized under various conditions of temperature, nitrogen overpressure and holding time with the help of X-ray diffraction (XRD), conventional TEM and EFTEM.

Experimental

The polyborosilazane with the internal designation T2-1 was prepared according Riedel et al. [1] by a two step synthesis (Fig. 1). First, the hydroboration of dichloromethylvinylsilane leads to tris(dichloromethylsilylethyl)borane (**a**), and secondly, the ammonolysis of the borane leads to the formation of polyorganoborosilazane (**b**). The synthesis procedures were performed in argon atmosphere using the Schlenk technique. Borane dimethyl sulfide (2 M solution in toluene) was obtained from Sigma Aldrich GmbH, Germany. Dichloromethylvinylsilane (ABCR GmbH, Germany) was distilled from Mg freshly before use. Tetrahydrofurane and toluene were purified by distillation from potassium.

For the synthesis of tris(dichloromethylsilylethyl)borane (**a**), 1,000 ml of a 2 M solution of $H_3B \cdot SMe_2$ was added at 0 °C in 6 h under vigorous stirring to a solution of 846 g (6 mol) dichloromethyvinylsilane in 900 ml toluene. The mixture was then stirred overnight at room temperature. After evaporation of SMe_2 and the solvent under reduced pressure, the compound was dried at 60 °C in vacuum (4 Pa). A colorless, oily liquid was obtained, with a yield of 870 g (99%). The synthesis of $(B[(C_2H_4)Si(CH_3)NH]_3)_n$ (**b**), with an internal designation T2-1, was carried out by dissolving 600 g (1.4 mol) of (**a**) in 900 ml tetrahydrofurane in a 4 l Schlenk flask consisting of gas inlet tube, mechanical stirrer, thermometer and reflux condenser. A stream of

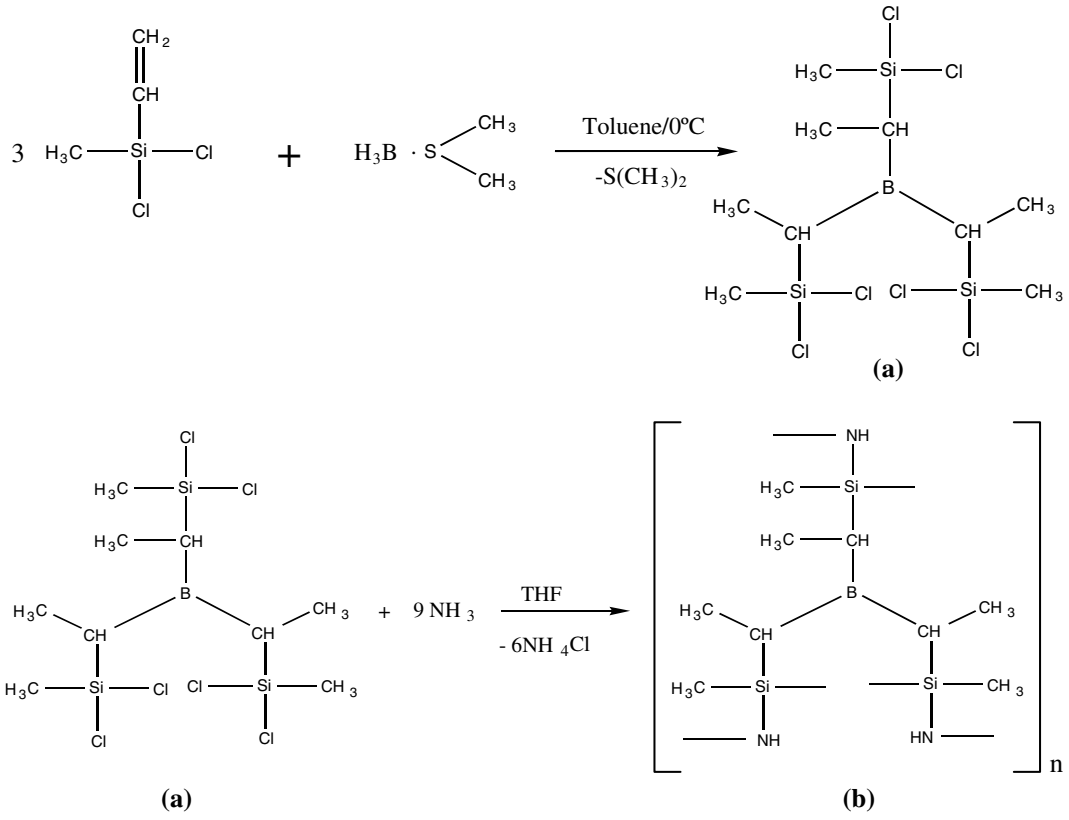

Fig. 1 Polymer synthesis procedure for the polyorganoborosilazane

ammonia was introduced under vigorous stirring. The temperature is raised up to the boiling point in 3 h; ammonia was introduced for 6 h. The mixture was filtered at room temperature through a Whatman glass microfibre filter (GF/D). The filtrate was concentrated and dried in vacuum (8×10^{-2} mbar) at 80 °C and 296.3 g (80%) of a white solid was obtained.

To obtain an infusible precursor a heat treatment to cross-link and a solid-state distillation to remove the remaining low molecular part was applied to (**b**). About 124 g of (**b**) was heated in a solid-state distiller for 1 h at 250 °C in argon at normal pressure, then heated up to 350 °C at reduced pressure (6 Pa) and kept at these conditions for 5 h. This distillation separates 44.2 g (35.6%) of distillate, a high viscous oil, from 74.1 g (59.7%) of residue, an infusible white preceramic solid. For the following experiments only the infusible part was used.

Consolidation of the preceramic particles in to green bodies was carried out using the warm pressing unit (Dr. Fritsch, DSP 475, Germany) in argon atmosphere. The green bodies were subjected to solid-state thermolysis at a temperature of 1,300 °C for 2 h in argon atmosphere. For the crystallization studies, annealing was carried out using a high temperature furnace (FCT, Germany) under a pressure of 1 MPa N_2. The following annealing treatments were carried out to study the influence of the temperature and holding time on the crystallization behavior: 1,800 °C/3 h, 1,900 °C/3 h and 1,800 °C/10 h. All heat treatments involved a heating rate of 10 K/min till 1,100 °C, 4 K/min till 1,300 °C and then 2 K/min up to the plateau temperature. A cooling schedule of 5 K/min till 1,300 °C followed by 20 K/min until room temperature was adopted.

The bulk density measurements of amorphous and their crystalline counterparts were performed by displacement measurements in mercury. Chemical analysis was performed using spectrochemical methods ELEMENTAR Vario EL, ELTRA CS 800 C/S determinator, LECO TC-436 N/O determinator and atomic emission spectrometry, ISA JOBIN YVON JY70 Plus. XRD measurements were carried out on the annealed specimens using a SIEMENS D5000 X-ray diffractometer with a position sensitive detector and CuKα radiation. For TEM observations, samples were prepared following standard techniques, which involve diamond cutting, ultrasonic drilling, mechanical grinding, dimpling, polishing and argon-ion thinning to perforation. TEM observations were made using a Philips CM200 microscope with an operating voltage of 200 kV. EFTEM was carried out using a Zeiss EM 912 Ω microscope with LaB_6 cathode operating at 120 kV. Data acquisition was performed with a Gatan 1024 X 1024 slow scan CCD camera. EFTEM was performed using the three-window method.

Results and discussion

The preceramic polymer precursor lumps were milled using a tungsten carbide ball mill and sieved into various size fractions. Particles in the size ranges 80–160 μm and 32–80 μm were separated and compacted in a graphite die at a uniaxial pressure of 48 MPa in the temperature range 250–340 °C. The warm pressing temperature needs to be optimized to get green bodies with a high density. To this end, the softening point of the polymer was determined by thermomechanical analysis. A plot showing the displacement in micrometers as a function of temperature is presented in Fig. 2. Tables 1 and 2 give details about the further optimization procedure. It is obvious that the optimum warm pressing temperature for the consolidation of the polymer particle size fractions 80–160 μm and 32–80 μm were 330 °C and 280 °C, respectively. Beyond which the ceramics would crack and break into pieces after thermolysis, as shown in Fig. 3. The cracks are a result of lack of residual open porosity in the ceramics, which are required for the evolution of the organic gaseous species.

Upon thermolysis, the preceramic polymer converts into a merely inorganic amorphous ceramic. Due to the evolution of organic gaseous species a weight loss of around 30% was observed during thermolysis which was independent of the size of the polymer particles used and independent of the warm pressing temperature. A continuous increase in density with increasing

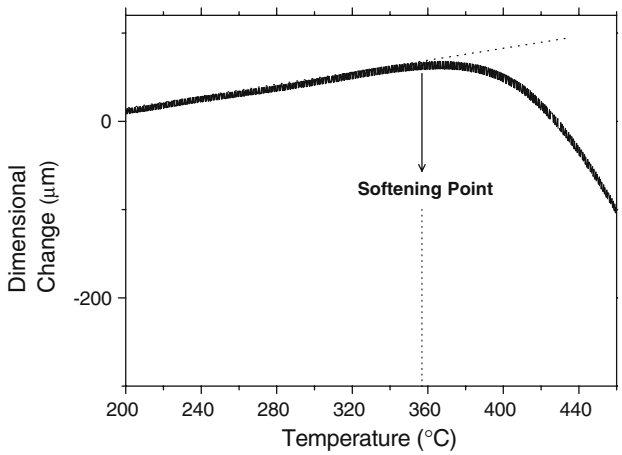

Fig. 2 Thermomechanical analysis of the polymer to determine the softening point

Table 1 Trial runs to determine the optimum warm pressing temperature for obtaining dense polymer green bodies, which can lead to crack free amorphous ceramics (polymer particles size range used is 80–160 μm)

Warm pressing temperature (°C)	Weight of green body (g)	Weight of pyrolyzed body (g)	Weight loss during pyrolysis (%)	Bulk density (g/cm^3)
250	1.992	1.4065	30	1.5663
280	1.992	1.4097	30	1.6786
320	2.500	1.7491	30	1.8446
330	1.649	1.1673	30	1.8917
340	Broken after pyrolysis			

Table 2 Trial runs to determine the optimum warm pressing temperature for obtaining dense polymer green bodies, which yield crack free amorphous ceramics (polymer particle size range used is 32–80 μm)

Warm pressing temperature (°C)	Weight of green body (g)	Weight of pyrolyzed body (g)	Weight loss during pyrolysis (%)	Bulk density (g/cm^3)
250	2.484	1.7477	30	1.92
280	2.505	1.7609	30	1.99
300, 320, 330	Broken after pyrolysis			

warm pressing temperature was observed in both cases. Maximum density values of around 1.89 g/cm^3 and 1.99 g/cm^3 without any noticeable cracks could be achieved after thermolysis of the green bodies obtained from the powder fractions 80–160 μm and 32–80 μm, respectively, i.e., the particle size has a pronounced influence on the result (Fig. 4). Earlier studies by Haug et al. [13] have shown that the mechanism of densification is the same for all the polymers investigated. At low temperatures some particle rearrangement occurs. With increase in temperature the particles soften, deform and melt together. However, as mentioned earlier, a fully densified green body has to be avoided since it does not yield a full dense ceramic, but would result in cracked and broken ceramic pieces after pyrolysis.

As observed in the histograms of Fig. 5, there was a weight loss of about 3% for materials derived from 80 μm to 160 μm particles and annealed at 1,800 °C for 3 h. Increasing the heat treatment temperature to 1,900 °C, a weight loss of 5.5% was recorded. For the same heat treatment conditions (1,900 °C, 3 h), the material produced using the smaller size fraction (32–80 μm) experienced a weight loss of 11% demonstrating a distinct influence of the size of the polymer particles. When the holding time was increased from 3 h to 10 h, materials annealed at 1,800 °C showed a weight loss of 4.3%. Similarly, exposing samples of polymer particles in the size range 32–80 μm under the same conditions, a weight loss of 8.5% was recorded. It was always observed that the weight loss was about doubled when the smaller size fraction of polymer particles were used for processing. This effect is thought to be due to the larger surface area to volume ratio at reduced particle size. The increase in density upon annealing was between 6% and 8.8% for the materials investigated, with the maximum increase occurring for the material annealed at 1,800 °C for 3 h. Increasing the temperature or holding time did not result in an appreciable increase in density.

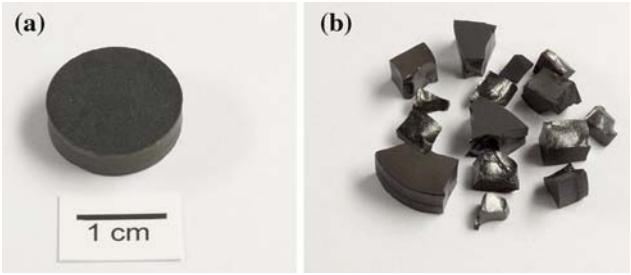

Fig. 3 Pyrolyzed amorphous Si–B–C–N ceramics (**a**) Bulk body obtained using optimum warm pressing temperature (T_{opt}) (**b**) Pieces broken when the warm pressing temperature was greater than the optimum warm pressing temperature ($T_{wp} > T_{opt}$)

Chemical analysis of tris(dichloromethylsilylethyl)borane yielded [wt% found (wt% calculated)]: Si 19.0 (19.2), B 2.5 (2.5), C 24.8 (24.7), H 4.3 (4.8), Cl 48.5 (48.7) and chemical analysis of the infusible solid polyorganoborosilazane yielded [wt% found (wt% calculated)]: Si 32.1 (31.3), B 4.2 (4.0), C 40.1 (40.1), N 15.7 (15.6), H 7.2 (8.9), O 0.8 (0.0). Chemical analyses were carried out for all crystallized samples too (Table 3); the resulting empirical chemical formulae for the materials are in the same order as in the table: $Si_{2.7}B_{1.0}C_{4.7}N_{2.1}$, $Si_{3.1}B_{1.0}C_{4.9}N_{2.02}$, $Si_{2.7}B_{1.0}C_{4.3}N_{1.2}$, $Si_{2.8}B_{1.0}C_{4.9}N_{2.1}$, and $Si_{2.9}B_{1.0}C_{4.6}N_{1.6}$. The crystallized materials mentioned in the table were prepared using polymer particles in the

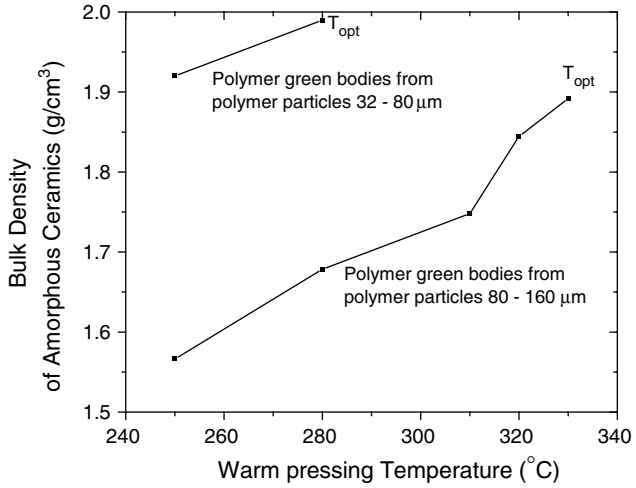

Fig. 4 Calculated bulk densities of amorphous ceramics as a function of warm pressing temperature used for consolidation of the polymer green bodies obtained from polymer particles in the range 80–160 μm and 32–80 μm. (T_{opt} is the maximum warm pressing temperature permissible for obtaining a dense crack free amorphous ceramic, beyond which the ceramic cracks, see Fig. 3.)

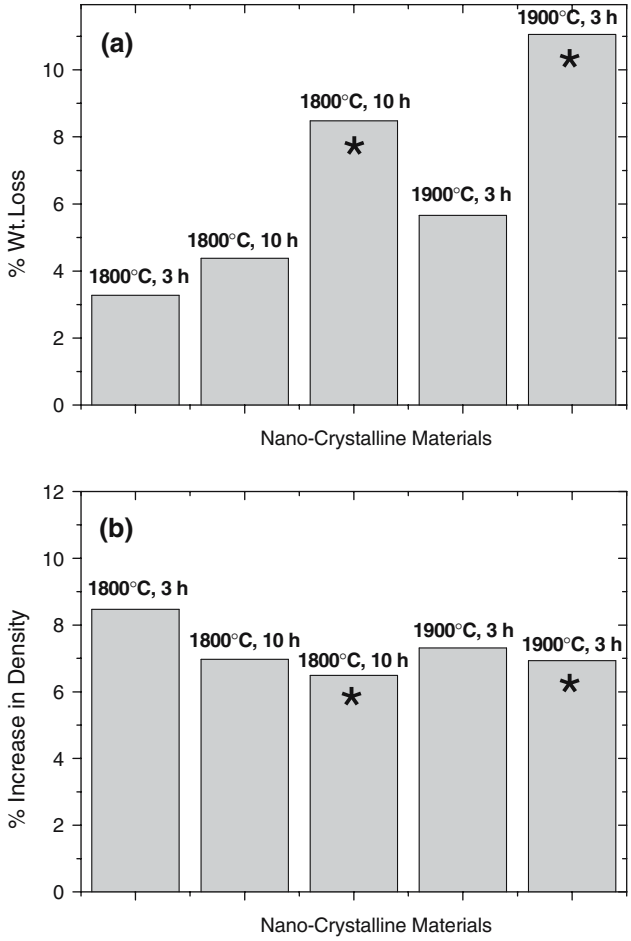

Fig. 5 Weight loss and increase in density of nano-crystalline Si–B–C–N ceramics after annealing for 3 h and 10 h at temperatures of 1,800 °C and 1,900 °C. All the materials were held at a constant overpressure of nitrogen of 1 MPa. The asterisk (*) indicate that the ceramics were synthesized using polymer particles in the size range of 32–80 μm

size range 80–160 μm, except for ones indicated by an asterisk (*), which were prepared using the 32–80 μm particles.

X-ray diffraction patterns were recorded as shown in Fig. 6, in concomitant with the transmission electron micrographs showing the structural features of the crystallized samples. The Bragg reflections correspond to SiC and Si_3N_4. The intensity of the silicon nitride peaks is reduced for the smaller polymer particles as a result of decomposition reactions. A broad peak corresponding to $2\theta = 25°–26°$ indicates the presence of turbostratic BN and C. Earlier XRD investigation of a ceramic obtained from BVT50, a boron containing polyvinylsilazane [14] indicated a peak at $2\theta = 25.8°$ besides the existence of β-SiC at 2,200 °C which was traced to a graphite-like turbostratic phase consisting of BN and C layers termed as BNC_x phase [15]. In the turbostratic structure individual layers of C and/or BN are stacked roughly parallel but with each layer having random orientation with regard to rotation about the layer normal. The formation of turbostratic layers has been detected by transmission electron microscopy in a number of polymer-derived materials including Si–C, Si–C–N [16, 17] and Si–B–C–N [18].

An analogous observation is made by energy filtering transmission electron microscopy (EFTEM), which was used to generate electron spectroscopic images

Table 3 Chemical analyses for all crystallized samples using various analytical techniques. (XRF = X-ray fluorescence spectroscopy, ICP-OES = Inductively coupled plasma – optical emission spectroscopy; "TC-436" and "Vario" are combustion techniques.)

Crystallized material	Si (wt %) XRF	B (wt %) ICP-OES	C (wt %) Vario	N (wt %) TC-436 & Vario	H (wt %.) Vario	O (wt %) TC-436
1,800 °C, 3 h—1 MPa N_2	43.8	6.15	32.10	16.9	< 0.1	1.3
1,900 °C, 3 h—1 MPa N_2	46.4	5.80	32.00	15.2	< 0.1	0.2
1,900 °C, * 3 h—1 MPa N_2	48.9	6.96	33.10	10.7	< 0.1	0.9
1,800 °C, 10 h—1 Mpa N_2	43.0	5.90	32.30	15.9	< 0.1	2.9
1,800 °C, * 10 h—1 MPa N_2	47.1	6.30	32.50	13.0	< 0.1	1.0

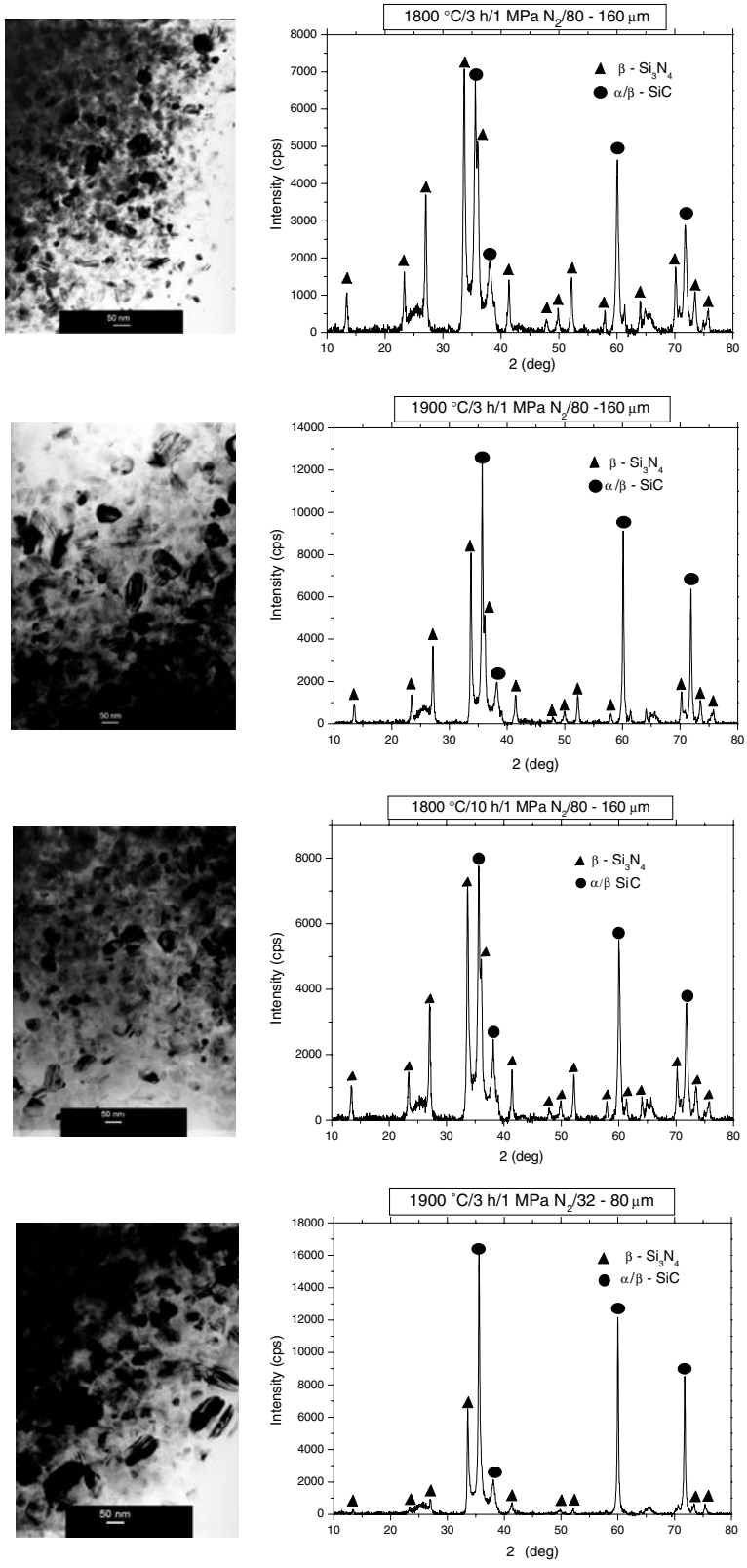

Fig. 6 XRD patterns along with TEM pictures of various crystallized Si–B–C–N ceramics showing the influence of annealing temperature, holding time and polymer particles size

showing the spatial distribution of elements in a qualitative manner. In the elemental maps shown in Fig. 7, the bright areas and dark areas show the presence and absence of a particular element. In most cases, grains appear dark and the surrounding matrix phase appears lighter in the bright field images also

included in Fig. 7, and it is just vice versa in the low loss images. With the help of the elemental maps of Si, B, C and N, it is possible to identify crystallites of SiC and Si_3N_4 unambiguously. The phase, which does not correspond to SiC and/or Si_3N_4, is obviously the BCN phase covering the crystallites. A close observation of TEM bright field and low loss images shows that the larger SiC crystallites identified by the Si and C elemental maps contain striped contrast features, which are caused by stacking faults as observed in Fig. 7b and c. This is in agreement with an earlier observation by Bunjes et al. [19]. Almost all large SiC crystals showed such striped contrast features and the stripes were always parallel to the longest axis of the 2-dimensional section of the grains. Si–B–C–N ceramics annealed at 1,800 °C for 3 h in nitrogen overpressure show a distribution of nano-crystallites of SiC and Si_3N_4. The nano-crystallites are predominantly spheroidal in morphology with an average crystallite size of around 50 nm (Fig. 7a). Increasing the holding time at 1,800 °C to 10 h results in a different nanostructure as shown in Fig. 7d. The nitrogen map reveals a significantly higher amount of nitrogen to be present in the material. Considering the Si, B, C and N maps collectively, one can confirm that there is a significant amount of Si_3N_4 in the material. Obviously, extending the holding time provides sufficient time for Si_3N_4 to crystallize. However, the extension of the holding time does not result in a drastic increase of the average crystallite size, and the grain morphology still remains spheroidal. On the contrary, annealing the material at the higher temperature of 1,900 °C for 3 h leads to grain growth to about 50–150 nm (Fig. 7b). Most of the crystallites are seen to be SiC, while the presence of Si_3N_4 is minimal. Extensive crystallization of SiC leaves behind but a thin residual layer of the BNC_x matrix phase.

A pronounced influence of the size of the polymer particles used for processing on the crystallization behavior is also observed. Si–B–C–N ceramics produced using polymer particles in the size range 32–80 μm (smaller size range) and annealed at 1,900 °C show elongated crystallites (Fig. 7c), which are identified to be SiC, while the elemental maps of Si, C and N do not show any Si_3N_4 crystals in the material. Some of the SiC crystallites are as large as 200 nm. In contrast, for the same annealing conditions, the material produced using 80–160 μm polymer particles (Fig. 7b) contains at least some Si_3N_4 crystals. Earlier studies on crystallization processes of amorphous Si–B–C–N ceramics indicated that annealing at temperatures higher than 1,800 °C leads to the formation of SiC

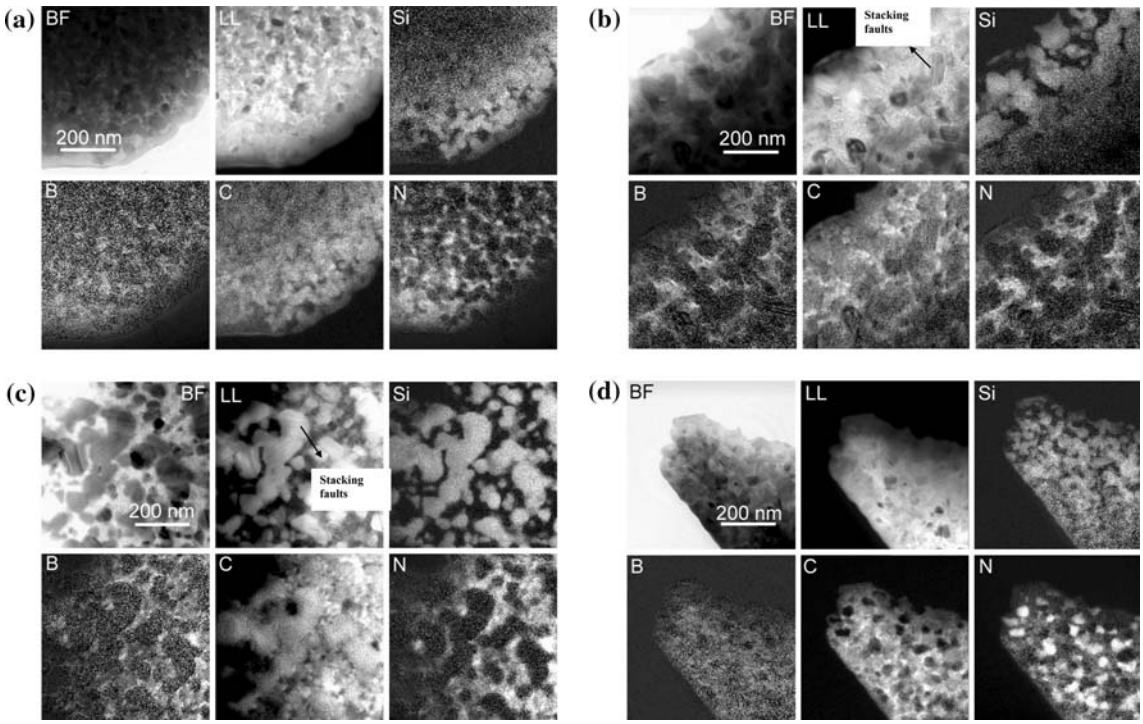

Fig. 7 Bright field (BF) and low loss images (LL) of Si–B–C–N ceramics crystallized at (**a**) 1,800 °C/3 h/1 MPa N_2 (80–160 μm), (**b**) 1,900 °C/3 h/1 MPa N_2 (80–160 μm), (**c**) 1,900 °C/3 h/1 MPa N_2 (32–80 μm), (**d**) 1,800 °C/10 h/1 MPa N_2 (80–160 μm) with their corresponding elemental maps

and Si_3N_4 with a mean grain size of 50 nm [20]. This crystallite size is much less than what is observed for boron-free materials under similar annealing conditions. As the size of the polymer particles used in the processing is reduced, the surface area to volume ratio is increased and the decomposition of Si_3N_4 is favored. The starting temperature of the decomposition is around 1,900 °C. This effect was also studied by Janakiraman et al. [11] where similar observations were reported, i.e., the extent of silicon nitride crystallization and its relative stability depend on the size of the polymer particles, the larger surface area of fine grained powders enabling vapor phase reactions that contribute to the decomposition of the materials. For a particle size larger than 315 μm a decomposition temperature of more than 2,000 °C was observed in [11], whereas a powder with a particle size between 32 μm and 80 μm decomposed at about 1,700 °C in agreement with the results obtained here.

Conclusions

- A highly crosslinked polymer precursor, boron modified poly(vinyl)silazane (T2-1) was synthesized and then subjected to solid-state thermolysis to obtain amorphous Si–B–C–N ceramics. Polymer particles in the size ranges of 32–80 μm and 80–160 μm were used. The processing conditions were optimized to obtain amorphous, crack free ceramic bodies with as high a density as possible, and it was observed that the optimum conditions are a function of the polymer particle size.
- Annealing of these amorphous ceramics at temperatures in the range of 1,800–1,900 °C yields crystallized ceramics with a microstructure consisting of SiC and Si_3N_4 crystallites distributed in a matrix of boron, nitrogen and carbon. A detailed characterization of the crystalline materials was undertaken by using chemical analysis, XRD, TEM and EFTEM. This is a precondition for selecting optimum crystallization conditions for producing materials with good mechanical characteristics and understanding their properties such as, e.g., high-temperature plasticity.

Acknowledgements The authors would like to acknowledge the technical support obtained for carrying out EFTEM and XRD from Ms. Ulrike Eigenthaler and Ms. Martina Thomas, respectively. The authors would also like to thank Dr. Anita Müller for fruitful scientific discussion.

References

1. Riedel R, Kienzle A, Dressler W, Ruwisch L, Bill J, Aldinger F (1996) Nature 382:796
2. Aldinger F, Weinmann M, Bill J (1998) Pure Appl Chem 70:439
3. Weinmann M, Kamphowe TW, Schuhmacher J, Muller K, Aldinger F (2000) Chem Mater 12:2112
4. Müller A, Gerstel P, Weinmann M, Bill J, Aldinger F (2000) J Eur Ceram Soc 20:2655
5. Riedel R, Ruwisch L, An L, Raj R (1998) J Am Ceram Soc 81:3341
6. Christ M, Thurn G, Weinmann M, Bill J, Aldinger F (2000) J Am Ceram Soc 83:3025
7. Christ M, Zimmermann A, Aldinger F (2001) J Mater Res 16:1994
8. Ravi Kumar NV, Mager R, Cai Y, Zimmermann A, Aldinger F (2004) Scripta Mater 51:65
9. Ravi Kumar NV, Prinz S, Cai Y, Zimmermann A, Aldinger F, Berger F, Müller K (2005) Acta Materialia 53(17):4567
10. Bauer A (2002) Dissertation an der Universität Stuttgart
11. Janakiraman N, Weinmann M, Schuhmacher J, Müller K, Bill J, Aldinger F, Singh P (2002) J Am Ceram Soc 85(7):1807
12. Zern A, Mayer J, Narayanan J, Weinmann M, Bill J, Rühle M (2002) J Eur Ceram Soc 22:1621
13. Haug R, Weinmann M, Bill J, Aldinger F (1999) J Eur Ceram Soc 19:1
14. Bill J, Kienzle A, Sasaki M, Riedel R, Aldinger F (1995) Adv Sci Tech 3B:1291
15. Peng J (2002) Dissertation an der Universität Stuttgart
16. Monthieux M, Delverdier O (1996) J Eur Ceram Soc 16:721
17. Jalowiecki A, Bill J, Fries M, Mayer J, Aldinger F, Riedel R (1995) Nanostruct Mater 6:279
18. Cai Y, Zimmermann A, Prinz S, Zern A, Phillipp F, Aldinger F (2001) Scripta Mater 45:1301
19. Bunjes N, Müller A, Sigle W, Aldinger F J Am Ceram Soc (accepted for publication)
20. Bill J, Kamphowe TW, Müller A, Wichmann T, Zern A, Jalowiecki A, Mayer J, Weinmann M, Schuhmacher J, Müller K, Peng J, Seifert HJ, Aldinger F (2001) Appl Organometal Chem 15:777